

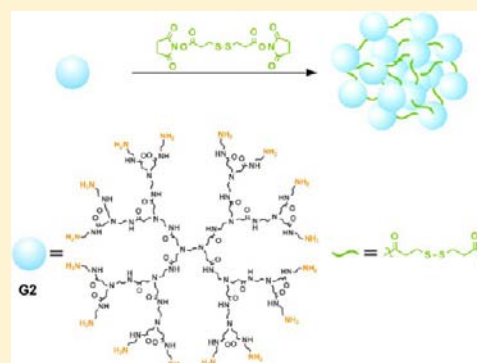
Disulfide Cross-Linked Low Generation Dendrimers with High Gene Transfection Efficacy, Low Cytotoxicity, and Low Cost

Hongmei Liu,[†] Hui Wang,[†] Wenjun Yang, and Yiyun Cheng*

Shanghai Key Laboratory of Regulatory Biology, School of Life Sciences, East China Normal University, Shanghai, 200241, PR China

S Supporting Information

ABSTRACT: Cationic poly(amidoamine) (PAMAM) dendrimers were widely used as nonviral gene carriers. PAMAM dendrimer-based products such as Superfect and Prifect were already commercially available gene transfection reagents. However, these products are based on high generation dendrimers with high cost and serious cytotoxicity. In this study, we prepared high efficient gene carriers using disulfide cross-linked low generation (generation 2, G2) PAMAM dendrimers. These synthesized materials can effectively condense DNA into ~200 nm polyplexes and degrade into G2 dendrimers after cellular uptake. Confocal laser scanning microscope studies revealed high cellular uptake behavior of disulfide cross-linked G2 PAMAM dendrimers. Compared to G2 and G5 PAMAM dendrimers, disulfide cross-linked G2 PAMAM dendrimers showed much improved gene transfection efficacy (both EGFP and luciferase gene) and low cytotoxicity on both HEK293 and HeLa cell lines. The disulfide cross-linked G2 dendrimer prepared at a linker/dendrimer molar ratio of 1:1 showed the highest gene transfection efficacy and exhibited comparable efficacy to branched PEI with a molecular weight of 25 kD, a commercially available nonviral gene vector. Our study demonstrated that disulfide cross-linked low generation PAMAM dendrimers with high transfection efficacy, low cytotoxicity, and low cost are efficient alternatives to high generation PAMAM dendrimers in gene delivery.



INTRODUCTION

Since polyamidoamine (PAMAM) dendrimers were first reported by Tomalia et al. in 1985,¹ these versatile polymers have steadily grown in popularity in miscellaneous fields, ranging from polymer chemistry to nanomedicine and biomaterials,^{2–6} especially in gene delivery. Numerous polymeric carriers for the delivery of DNA and siRNA were developed as alternatives to viral carriers in the past decade.^{6–9} Amine-terminated PAMAM dendrimers have well-defined numbers of primary amine and tertiary amine groups on the surface or in the interior.¹⁰ The surface amine groups with pK_a values around 10.0 are protonated at physiological condition, endowing these polymers with the ability to bind negatively charged DNA molecules.^{11,12} Cationic surface of PAMAM dendrimers combined with their flexible structure and nano-scale size (1–10 nm) mean they can easily condense DNA molecules into polyplexes.^{13,14} In addition, efficient cellular uptake of PAMAM dendrimers and dendrimer/DNA polyplexes were reported on different cell lines, and the polyplexes were mainly localized within endosomes after cellular uptake.^{15–17} Tertiary amine groups in the interior pockets of PAMAM dendrimers with pK_a values around 6.0 have pH buffering ability, which enhances the endosomal escape of the polyplexes.^{11,18} Furthermore, PAMAM dendrimers are non-immunogenic, thus reducing the safety risks of viral vectors in gene delivery.⁴ PAMAM dendrimers were shown to be as efficient as liposomes and other cationic polymers such as polyethylenimine (PEI).¹⁹ Because of these properties,

PAMAM dendrimers are safe and efficient alternatives to viral, lipid, and polymeric gene vectors. Up to now, PAMAM dendrimer-based products such as Superfect and Prifect (Starpharma) were already commercially available gene transfection reagents.

However, PAMAM dendrimer-based gene transfection reagents are involved with several challenges. (1) High cost of high generation dendrimer: the synthesis of high generation PAMAM dendrimer is labor-consuming, and the costs of PAMAM-related products are more expensive than other cationic polymers. Although recently developed click chemistry allows the synthesis of high generation PAMAM dendrimers within a couple of days,²⁰ reducing the cost of PAMAM-based product remains a major challenge in a near future. (2) The transfection efficacy and cytotoxicity paradox: high generation PAMAM dendrimers possess relatively high gene transfection efficacy but serious cytotoxicity to transfected cells, while low generation dendrimers have low transfection efficacy and low cytotoxicity.^{4,19} However, ideal gene transfection reagents should have high transfection efficacy and low cytotoxicity. To achieve higher gene transfection efficacy, high generation PAMAM dendrimers were functionalized with hydrophobic chains such as aliphatic acid,²¹ and amino acids including arginine,^{22,23} lysine,²³ phenylalanine,²⁴ leucine,²⁴ and proline²⁵ to tailor the dendrimer surface charge and hydrophobicity, with

Received: July 25, 2012

Published: October 10, 2012

Scheme 1. Synthetic Route of the G2DSPs by Cross-Linking G2 PAMAM Dendrimers Using a Reducing Degradable DSP Linker

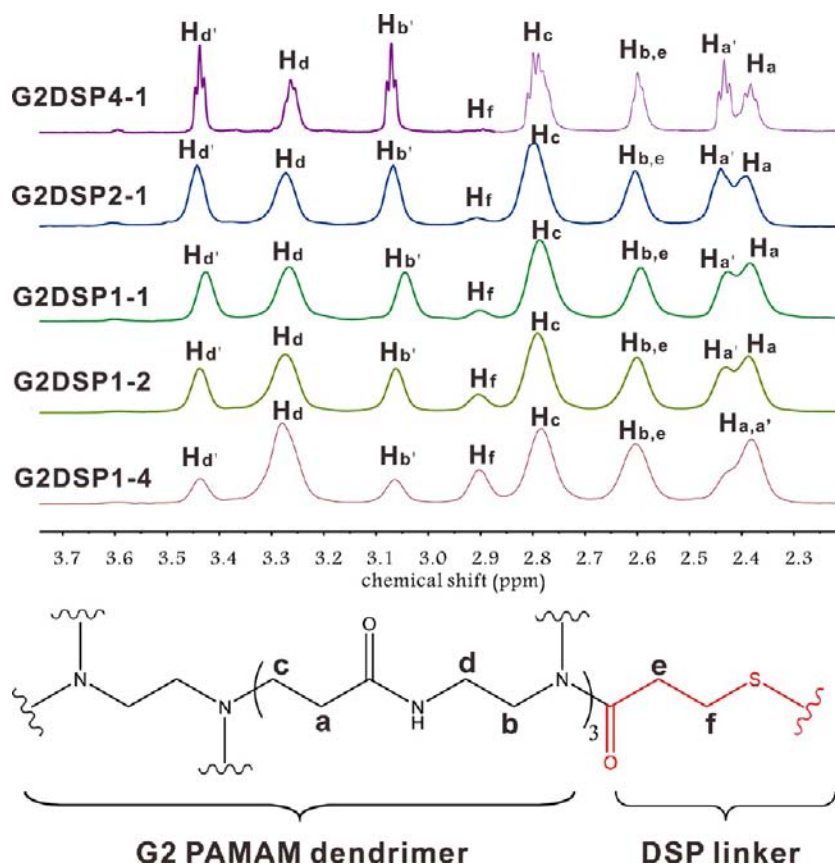
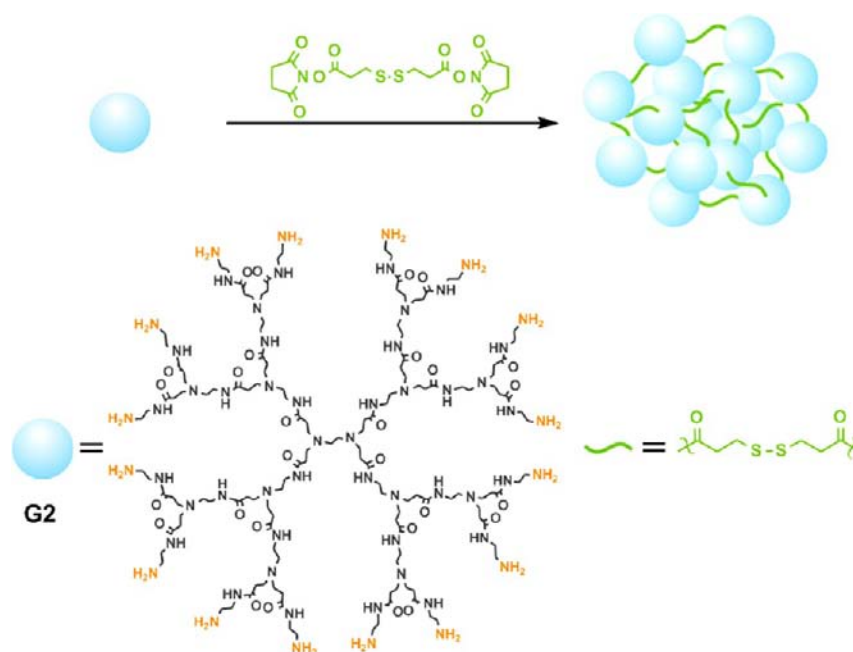


Figure 1. ^1H NMR spectra of the synthesized G2DSPs (G2DSP4-1, G2DSP2-1, G2DSP1-1, G2DSP1-2, and G2DSP1-4) in D_2O . The chemical structure of the synthesized G2DSPs with proton labeling is shown in the bottom row.

targeting moieties such as folic acid,²⁶ mannose,²⁷ lactose,²⁸ galactose,²⁹ biotin,³⁰ transferrin,³¹ and peptides,³² with pH-buffering compounds such as guanidine and spermine,²⁵ and with nanoparticles such as carbon nanotubes and gold

nanoparticles.^{33–35} These strategies can efficiently improve the transfection efficacy of PAMAM dendrimers. However, high transfection efficacy is usually accompanied with high cytotoxicity in these gene delivery systems. Therefore, there

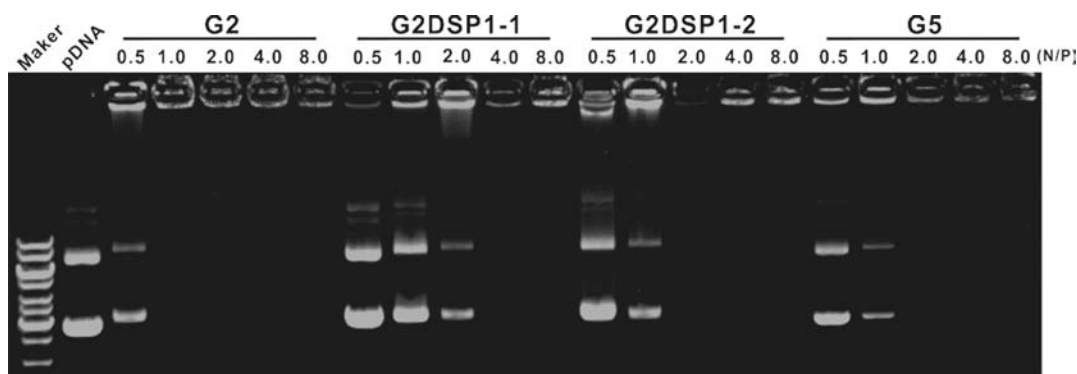


Figure 2. Agarose gel electrophoresis assay of G2, G2DSP1–1, G2DSP1–2, G5 polyplexes with EGFP plasmid. Lane 1 and lane 2 correspond to marker and naked plasmid DNA. Lanes 3–7 represent G2/DNA polyplexes with N/P ratios of 0.5:1, 1:1, 2:1, 4:1, and 8:1, respectively. Lanes 8–12 represent G2DSP1–1/DNA polyplexes with N/P ratios of 0.5:1, 1:1, 2:1, 4:1, and 8:1, respectively. Lanes 13–17 represent G2DSP1–2/DNA polyplexes with N/P ratios of 0.5:1, 1:1, 2:1, 4:1, and 8:1, respectively. Lanes 18–22 represent G5/DNA polyplexes with N/P ratios of 0.5:1, 1:1, 2:1, 4:1, and 8:1, respectively.

is an urgent need to break up the correlation between transfection efficacy and cytotoxicity for cationic dendrimer-based gene vectors.³⁶ A solution to this problem is the preparation of high efficient gene transfection reagents using low generation dendrimers. In the past decade, Uekama et al. developed cyclodextrin-modified low generation PAMAM dendrimers for DNA and siRNA delivery.^{27–29,37} In their studies, relatively high gene transfection efficacy and low cytotoxicity of the cyclodextrin–dendrimer conjugates were achieved.

In this study, we proposed a new strategy in the preparation of highly efficient gene carriers using low generation PAMAM dendrimers. Disulfide containing linker (3,3'-dithiodipropionic acid-di(*N*-succinimidyl ester), DSP) was used to cross-link generation 2 (G2) PAMAM dendrimers to form supramolecular structures (G2DSPs). The disulfide bond reduction usually occurs in the endocytic pathway.^{36,38} This means the DSP cross-linked G2 PAMAM dendrimers can be degraded to G2 PAMAM monomolecules after gene transfection, and the resulting G2 PAMAM dendrimer can minimize the damage of cationic gene transfection reagents to transfected cells. The goal of this study is to prepare low generation PAMAM dendrimer-based gene vectors with low cost, low cytotoxicity, and high gene transfection efficacy.

RESULTS AND DISCUSSION

Characterizations of G2DSPs and G2DSPs/DNA Polyplexes. G2DSPs were synthesized according to Scheme 1. To optimize the synthesized G2DSPs, five molar ratios of G2 PAMAM dendrimer to DSP (1:4, 1:2, 1:1, 2:1, and 4:1) were chosen. The products are termed as G2DSP1–4, G2DSP1–2, G2DSP1–1, G2DSP2–1, and G2DSP4–1, respectively. The synthesized materials were characterized by ¹H NMR and COSY spectra. As shown in Figure 1, G2DSPs show characteristic peaks for G2 PAMAM dendrimer (H_{a-d} for G2 scaffold methylene protons, H_b , and H_d for G2 surface methylene protons adjacent to protonated NH_2 groups).⁵ With the help of COSY spectrum in Figure S1 (Supporting Information), resonance assignments of protons in the DSP linker were simplified (H_e and H_f , H_e is overlapped with H_b of G2 PAMAM dendrimer). It is clearly observed in Figure 1 that the signal intensity of H_f increases with the molar ratio of DSP to G2 PAMAM. On the basis of the peak areas of H_f and H_e in Figure 1, the ratio of DSP to G2 in G2DSP1–1 is calculated to

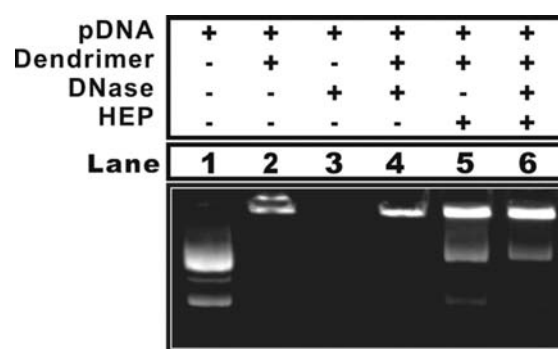


Figure 3. DNase protection assay. Lane 1, EGFP plasmid DNA. Lane 2, G2DSP1–1/DNA polyplexes at an N/P ratio of 8:1. Lane 3, EGFP DNA treated with DNase for 2 h. Lane 4, G2DSP1–1/DNA polyplexes at an N/P ratio of 8:1 was treated with DNase for 2 h. Lane 5, release the DNA bound by G2DSP1–1 using heparin. Lane 6, G2DSP1–1/DNA polyplexes treated with DNase for 2 h, followed by heat-inactivation of the DNase, and release of the bound DNA using heparin.

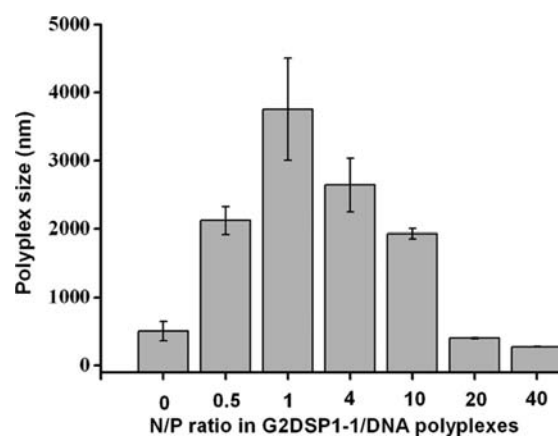


Figure 4. Hydrodynamic sizes of G2DSP1–1/DNA polyplexes at different N/P ratios determined by dynamic light scattering.

be 1.3, which is similar to the DSP and G2 feeding ratio, suggesting that most of the DSP linkers participate in the formation of G2DSPs. It is worth noting the possibility of intracellular cross-linking in the synthesized G2DSPs when using homobifunctional cross-linking agents. Since DSP is

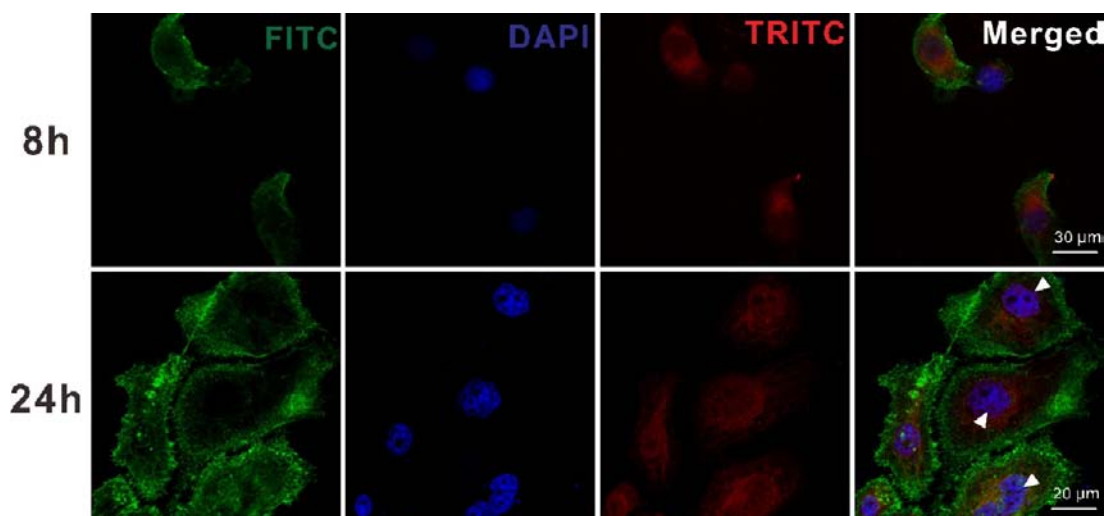
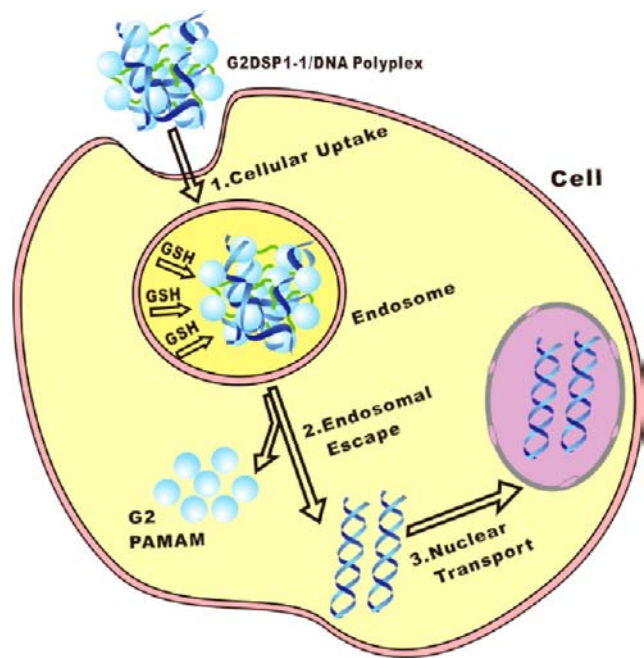


Figure 5. Confocal microscopic images of HeLa cells treated with G2DSP1-1-TRITC for 8 and 24 h. The actin filaments were stained with phalloidin-FITC, and the nuclei were stained with DAPI. The arrows indicate the colocalization of TRITC and DAPI within the nuclei of HeLa cells.

Scheme 2. Proposed Mechanism of G2DSP1-1 in the Delivery of DNA Molecules into Cell Nucleus



slowly titrated into high concentration G2 dendrimer solutions, considering the excess amount of amine groups during the reactions, the short chain length of DSP, and the energy unfavorable structure of intramolecular cross-linking, intermolecular cross-linking should be the predominant form in the resulting G2DSPs. Since G2DSP1-1 shows the highest gene transfection efficacy among the synthesized G2DSPs in later gene transfection experiments, it was conjugated with a fluorescent dye (tetramethylrhodamine isothiocyanate, TRITC) to investigate the cellular uptake and localization behaviors of the material. The ^1H NMR spectrum of G2DSP1-1-TRITC is shown in Figure S2 (Supporting Information). By integrating the peak areas of TRITC methyl protons and G2 PAMAM methylene protons, an average number of 1.1 TRITC molecules were conjugated to each G2 PAMAM dendrimer.

UV-vis spectrum of G2DSP1-1-TRITC in Figure S3 (Supporting Information) further confirms the conjugation of TRITC molecules to the surface of PAMAM dendrimer.

To investigate the optimal N/P ratio of G2DSPs/DNA polyplexes, the complexes were prepared at different N/P ratios (0.5:1 to 8:1), and the electrophoretic mobility of DNA in the polyplexes was analyzed in an agarose gel in comparison with G2 and G5 PAMAM dendrimers. As shown in Figure 2, G2 and G5 PAMAM dendrimers form stable polyplexes with DNA above the N/P ratio of 1:1, while G2DSP1-1 condenses DNA into polyplexes above the N/P ratio of 2:1. The lower efficacy of G2DSP1-1 in the condensation of DNA is due to the presence of unreachable NH_2 groups in the supramolecular structure of G2DSP1-1 (Scheme 1).

The protection of DNA against DNase by G2DSP1-1 is shown in Figure 3. To achieve successful entry of DNA in a cell, its protection from DNase is essential since the DNase can rapidly degrade free DNA molecules during the transfection process. Naked DNA was degraded in the presence of DNase within 2 h, while the DNA complexed with G2DSP1-1 at an N/P ratio of 8:1 can protect the DNA from degradation. The bound DNA in the G2DSP1-1/DNA polyplexes can be released by the addition of heparin, a polyanion molecule. In the presence of heparin, still a high percent of DNA were recovered after the incubation of G2DSP1-1/DNA polyplexes with DNase for 2 h. These results clearly suggest that G2DSP1-1 can effectively protect DNA from degradation.

The hydrodynamic size of G2DSP1-1 is measured to be 40 nm, which is much larger than the molecular size of G2 PAMAM dendrimer. G2DSP1-1 was able to condense DNA into nanoparticles with an average size of 2100 nm at an N/P ratio of 0.5:1. The largest polyplex size (3800 nm) is achieved at an N/P ratio of 1:1, and the particle size decreases until the N/P ratio of 40:1 (Figure 4). At the N/P ratio of 40:1, the average size of G2DSP1-1/DNA polyplexes is 275 nm. Polyplexes with a size around 200 nm were proved to be suitable for gene transfection in the references.^{12,30,39} In addition, the polyplex size is scarcely changed when the polyplex solution is diluted, indicating the stability of G2DSP1-1/DNA polyplexes.

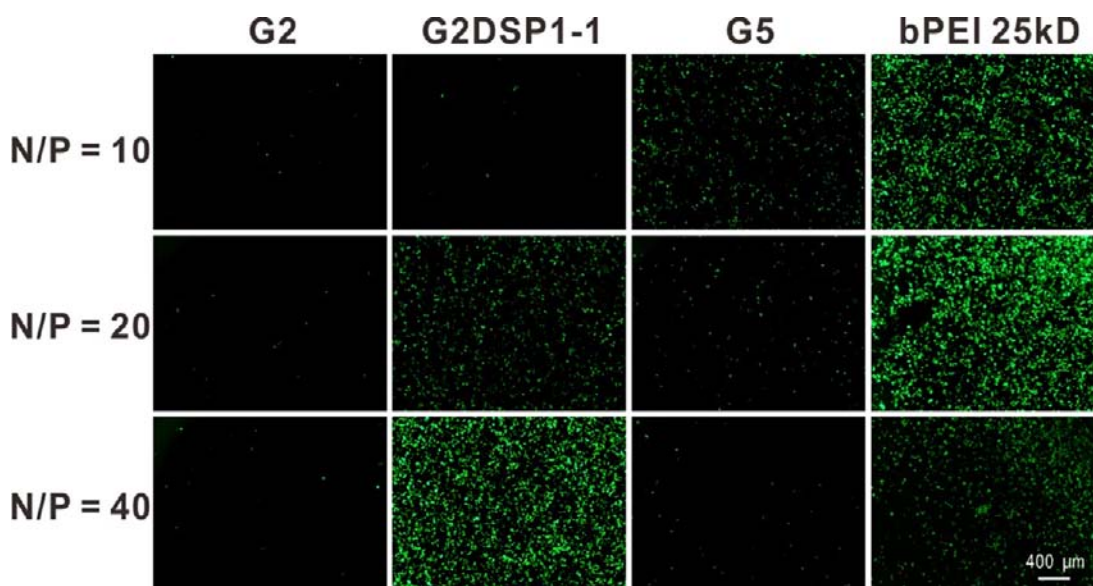


Figure 6. Fluorescent microscopy images of HEK293 cells transfected by G2, G2DSP1-1, G5, and bPEI 25 kD for 24 h. EGFP plasmid expressions in HEK293 cells were observed in green fluorescence. The N/P ratios of the polyplexes were 10:1, 20:1, and 40:1, respectively.

Cellular Uptake and Intracellular Localization of G2DSP1-1. The cellular uptake and intracellular localization of a gene carrier play important roles in successful gene transfection. To determine the intracellular behaviors of G2DSP1-1 after cellular uptake, HeLa cells were incubated with G2DSP1-1-TRITC and observed by fluorescence microscopy and laser scanning confocal microscopy (CLSM). Red fluorescence was observed in HeLa cells within 2 h of incubation (data not shown). As shown in Figure S4 (Supporting Information), the fluorescence appears punctuate and is observed intracellular. Nearly 100% of the cells were observed with fluorescently labeled G2DSP1-1, suggesting efficient cellular uptake of the material. To further determine the localization of G2DSP1-1-TRITC after cellular uptake, DAPI (blue) was used to stain the nucleus and phalloidin-FITC (green) was used to stain actin filaments. As shown in Figure 5, red fluorescence (TRITC) was only observed in the cytoplasm at 8 h, but was observed both in the cytoplasm and inside the nucleus after 24 h of incubation. It is reported that the concentration of intracellular glutathione (GSH) is 100–1000 times higher than extracellular GSH.³⁶ Therefore, the disulfide bond among G2 PAMAM dendrimers in G2DSP1-1 is degradable in cell cytoplasm, endosomes, and lysosomes (Scheme 2). Since G2DSP1-1 has a relatively large hydrodynamic size around 40 nm, the colocalization of TRITC and DAPI in Figure 5 indicates the degradation of G2DSP1-1-TRITC to G2-TRITC within the cells after 24 h of incubation. These observations clearly demonstrate the high cellular uptake ability of G2DSP1-1 and the degradation of G2DSP1-1 after cellular uptake.

In Vitro Transfection Efficacy of G2DSPs. After demonstrating the efficient cellular uptake of G2DSPs, in vitro gene transfection efficacy of G2DSPs was measured with EGFP gene on HEK293 and HeLa cells and with luciferase gene on HEK293 cells. Among the five synthesized materials, G2DSP1-1 shows much higher gene transfection efficacy than G2DSP2-1, G2DSP1-2, and G2DSP1-4 at different N/P ratios (Figure S5, Supporting Information). For G2DSP4-1 and G2DSP2-1, partial G2 dendrimers are not cross-linked

with others because of the relatively low DSP/G2 ratios. In comparison, G2 dendrimers are cross-linked into large size aggregates in G2DSP1-2 and G2DSP1-4. As a result, G2 and DSP ratio of 1:1 is the optimal ratio in the preparation of gene vectors, and G2DSP1-1 was investigated in detail in further gene transfection and cytotoxicity studies. As shown in Figure 6 and Figure S6 (Supporting Information), the exogenous EGFP transfection efficacy increases with the N/P ratio and polyplex incubation time for G2DSP1-1/EGFP polyplexes. They exhibited low EGFP gene expression in HEK293 cells at an N/P ratio of 10:1 but high EGFP expressions at N/P ratios of 20:1 and 40:1. It is obvious that the gene expressions of G2DSP1-1/EGFP polyplexes at 20:1 and 40:1 are much higher than that of G2/EGFP and G5/EGFP polyplexes at all the N/P ratios. Unlike G2DSP1-1, G5 shows highest transfection efficacy at N/P ratio of 10:1. The low transfection efficacies of G5 at N/P ratios of 20:1 and 40:1 are due to the cytotoxicity of G5 at high concentrations. In addition, G2DSP1-1 at an N/P ratio of 40:1 exhibits comparable EGFP transfection efficacy with branched PEI with a molecular weight of 25 kD (bPEI 25 kD) at an optimal N/P ratio of 10:1. Similar results were observed in Figure S7 (Supporting Information) for HeLa cells.

To check if the disulfide bond in G2DSP1-1 is essential for its high gene transfection efficacy, G2DSP1-1 was incubated with 5 equiv of DTT before complexation with EGFP gene, and the EGFP transfection was observed with fluorescence microscopy. DTT treated G2DSP1-1 restored its ability in binding EGFP gene (Figure S8, Supporting Information); however, G2DSP1-1 showed extremely low EGFP transfection efficacy in the presence of DTT in both HEK293 and HeLa cells (Figure 7a), suggesting that the disulfide bond in the G2DSP1-1 can be reduced and the disulfide cross-linking plays an important role in gene transfection. To confirm the importance of disulfide cleavage in G2DSP1-1 during gene transfection, disuccinimidyl suberate (DSS) without disulfide bond was used to cross-link G2 PAMAM dendrimer at a DSS/G2 molar ratio of 1:1 (Figure 7b), and the gene transfection efficacy of G2DSS1-1 was evaluated using EGFP as a reporter

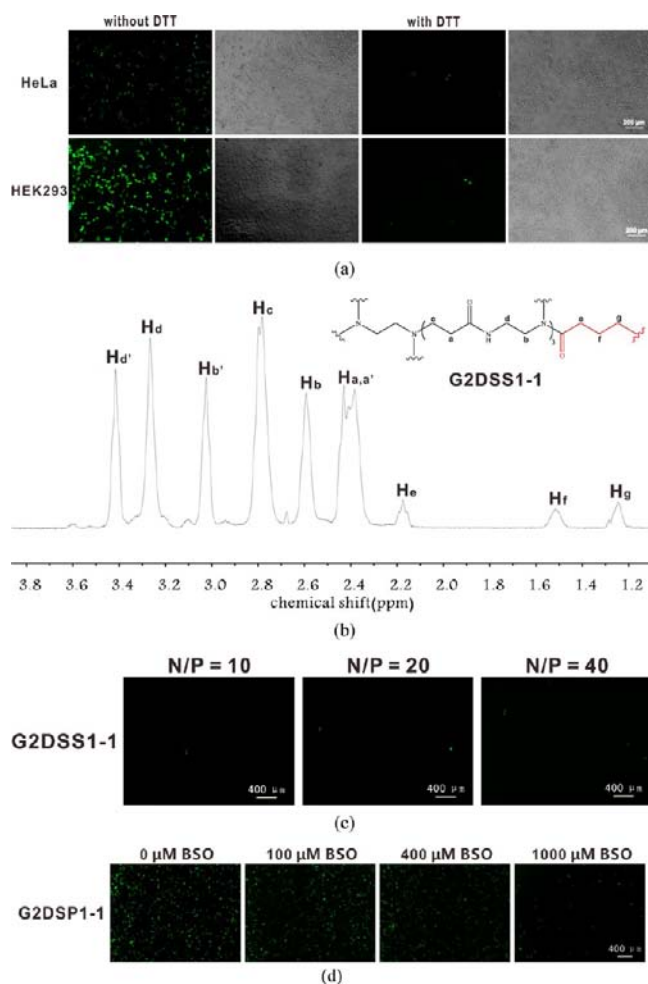


Figure 7. (a) Fluorescent microscopy images of HeLa and HEK293 cells transfected by G2DSP1-1 for 24 h. G2DSP1-1 was treated without or with 5 equiv of DTT before complexation with EGFP gene. The N/P ratio of the polyplexes was fixed at 40:1. (b) ¹H NMR spectrum of G2DSS1-1 in D₂O with chemical shift assignments. (c) EGFP gene expression of G2DSS1-1/EGFP polyplexes at N/P ratios of 10:1, 20:1, and 40:1, respectively. (d) EGFP Gene transfection efficiency of G2DSP1-1 in the presence of different amounts of BSO.

gene. As shown in Figure 7c, extremely low EGFP gene expressions were observed for G2DSS1-1/EGFP polyplexes at N/P ratios of 10:1, 20:1, and 40:1, suggesting that disulfide cleavage is essential for high gene transfection efficacy of G2DSP1-1. The inhibition of disulfide cleavage in G2DSP1-1 during gene transfection by DL-buthionine sulfoximine (BSO), a GSH depletor, also caused significantly decreased EGFP expression of G2DSP1-1/EGFP polyplexes (Figure 7d). These results together confirm the importance of disulfide cleavage in G2DSP1-1 during gene transfection.

To quantitatively compare the transfection efficacy of G2DSP1-1, G2, G5, and bPEI 25 kD, we use flow cytometry to determine the percent of positive cells transfected with EGFP gene. As shown in Figure 8a and Figure S9 (Supporting Information), G2DSP1-1 transfected 0.18, 16.91, and 34.8% HEK293 cells at N/P ratios of 10:1, 20:1, and 40:1, respectively. In comparison, naked EGFP gene shows 0% transfection efficacy in HEK293 cells. G2 PAMAM exhibits 0.18, 0.16, and 0.15% efficacies at N/P ratios of 10:1, 20:1, and 40:1, respectively, while the values for G5 PAMAM dendrimer are 10.58, 4.00, and 1.83%, respectively. bPEI 25 kD at an

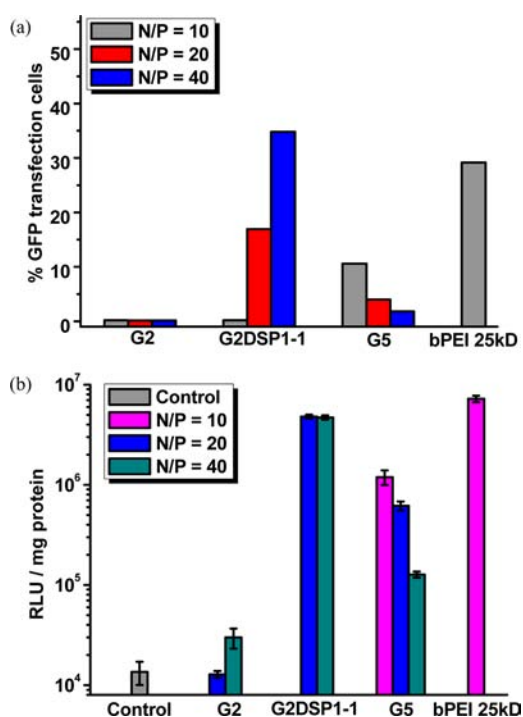


Figure 8. Comparison of G2DSP1-1 with G2, G5, and bPEI 25 kD on in vitro EGFP gene (a) and luciferase gene (b) transfection efficacy in HEK293 cells. The EGFP gene transfection efficacy (%) was determined from flow cytometry, and the luciferase gene expression level is expressed as relative luciferase light units (RLU)/mg of protein.

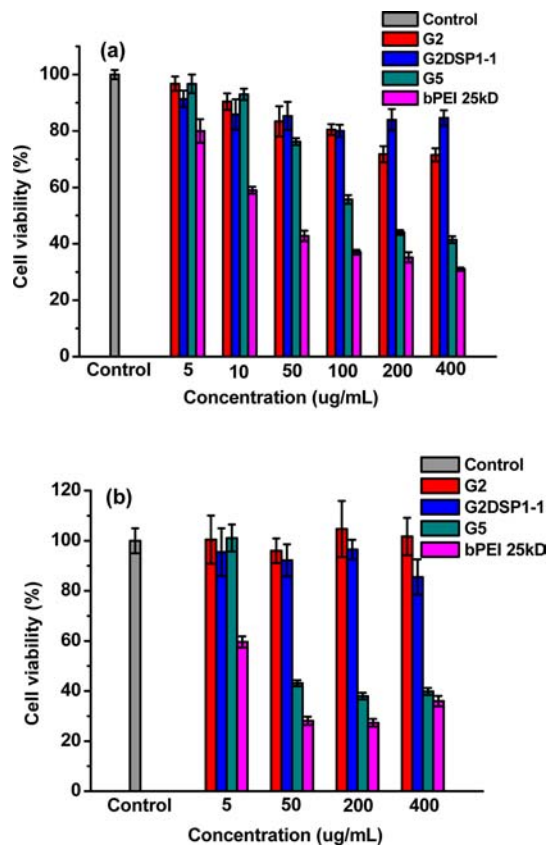


Figure 9. Comparison of G2DSP1-1 cytotoxicity on HeLa (a) and HEK293 (b) cells with the cytotoxicities of G2, G5 and bPEI 25 kD.

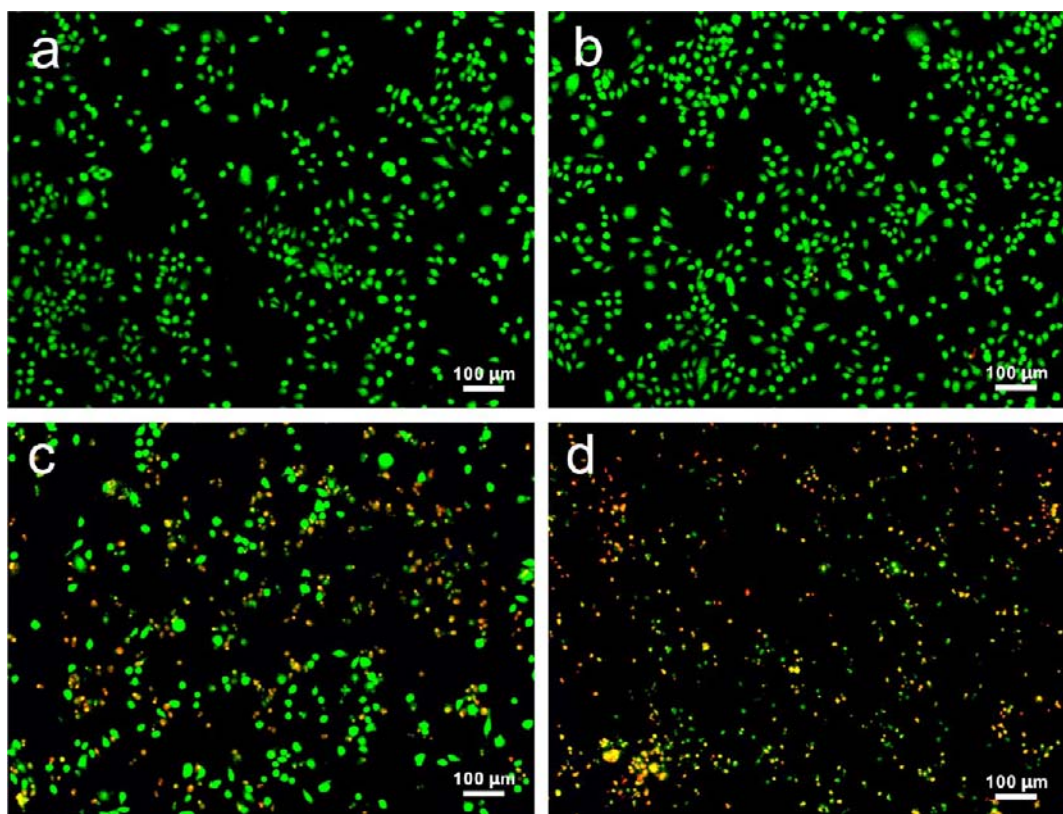


Figure 10. Images of HeLa cells incubated with (a) 200 $\mu\text{g}/\text{mL}$ of G2 PAMAM, (b) 200 $\mu\text{g}/\text{mL}$ of G2DSP1-1, (c) 200 $\mu\text{g}/\text{mL}$ of G5 PAMAM, and (d) 100 $\mu\text{g}/\text{mL}$ of bPEI 25 kD in an AO/EB assay.

optimal N/P ratio of 10:1 shows a 29.17% EGFP gene transfection efficacy in HEK293 cells. These results are in accordance with that observed by the fluorescence microscopy (Figure 6). The other synthesized polymers G2DSP4-1, G2DSP2-1, G2DSP1-2, and G2DSP1-4 showed much lower transfection efficacy in the flow cytometry studies compared to G2DSP1-1. Among these materials, G2DSP1-4 shows the highest transfection efficacy of 11.12% at an N/P ratio of 40:1 (data not shown).

Transfection efficacies of G2DSP1-1, G2, G5, and bPEI 25 kD polyplexes with luciferase gene were further investigated, as shown in Figure 8b. G2DSP1-1 shows comparable luciferase gene expression efficacy with bPEI 25 kD, and much higher efficacy than naked DNA, G2, and G5 PAMAM dendrimers. Other synthesized G2DSPs show lower luciferase gene expression than G2DSP1-1 (Figure S10, Supporting Information), which is in accordance with the results in EGFP gene transfection experiments. These results confirm that G2DSP1-1 can be used as a promising nonviral gene vector.

Cytotoxicities of G2DSPs and G2DSPs/DNA Polyplexes. MTT assay was carried out to evaluate the cytotoxicities of G2DSPs. G2DSP1-1 exhibits high cell viability (>80%) on HEK293 and HeLa cells at concentrations up to 400 $\mu\text{g}/\text{mL}$ and is even more biocompatible than G2 PAMAM dendrimers on HeLa cells at 200 and 400 $\mu\text{g}/\text{mL}$ (Figure 9). Other synthesized G2DSPs also showed low cytotoxicity on these cells (Figure S11, Supporting Information). In comparison, G5 PAMAM and bPEI 25 kD show significant cytotoxicity on HeLa and HEK293 cells (<50% cell viability at 200 and 50 $\mu\text{g}/\text{mL}$ for G5 and PEI, respectively). In addition, the complexation of G2DSP1-1 with DNA does not cause additional cytotoxicity to the cells (Figure S12, Supporting

Information). The biocompatibility of G2DSP1-1 is further confirmed by an AO/EB assay. AO is able to penetrate through the cell membranes of normal and necrotic cells, while EB is only taken by necrotic cells with damaged membranes, resulting in bright green and orange fluorescence on the normal and necrotic cells, respectively.⁴⁰ As shown in Figure 10, G2DSP1-1 and G2 PAMAM dendrimer (200 $\mu\text{g}/\text{mL}$) treated HeLa cells were only observed with green fluorescence, while G5 PAMAM (200 $\mu\text{g}/\text{mL}$) and bPEI 25 kD (100 $\mu\text{g}/\text{mL}$) treated cells were observed with both green and red fluorescence. The degradation product of G2DSP1-1 in the presence of DTT shows similar biocompatibility to G2 PAMAM dendrimer (Figure S13, Supporting Information), suggesting that the presence of thiol terminal groups on G2 dendrimer does not cause additional cytotoxicity to G2 dendrimer. These results together suggest that G2DSP1-1 has relatively high gene transfection efficacy and is able to maintain the high cell viabilities at the same time.

CONCLUSIONS

In the present study, we synthesized a new class of disulfide cross-linked G2 PAMAM dendrimers for the design of high efficient and low cytotoxic gene carriers. Among the synthesized materials, G2DSP1-1 shows higher gene transfection efficacy than G2 and G5 PAMAM dendrimers and comparable efficacy with bPEI 25 kD and is more biocompatible than these cationic polymers. The results indicate that regulated release of DNA through polymer degradation is a critical step for efficient gene transfection.³⁸ G2DSP1-1, with high transfection efficacy, low cytotoxicity, and low cost, is proposed to be a promising nonviral gene

carrier based on PAMAM dendrimers. We are now optimizing the transfection efficacy of cross-linked low generation dendrimers by varying dendrimer generations, cross-linking reagents, dendrimer components, as well as linker/dendrimer molar ratios. The transfection efficacies and cytotoxicities of these materials will be discussed in detail in the forthcoming work.

■ ASSOCIATED CONTENT

■ Supporting Information

Figures S1–S17. Further data on characterization of the G2DSPs and G2DSPs/DNA polyplexes, in vitro gene transfection efficacy, and cytotoxicity of G2DSPs. This material is available free of charge via the Internet at <http://pubs.acs.org>.

■ AUTHOR INFORMATION

Corresponding Author

yycheng@mail.ustc.edu.cn

Author Contributions

[†]These authors contributed equally on this manuscript.

Notes

The authors declare no competing financial interest.

■ ACKNOWLEDGMENTS

We are thankful for financial support from the Science and Technology of Shanghai Municipality (11DZ2260300), the “Dawn” Program of Shanghai Education Commission (No. 10SG27), the Program for New Century Excellent Talents in University of Ministry of Education of China, and the Innovation Program of Shanghai Municipal Education Commission (No. 12ZZ044) on this project.

■ REFERENCES

- (1) Tomalia, D. A.; Baker, H.; Dewald, J.; Hall, M. G. K.; Martin, S.; Roeck, J.; Ryder, J.; Smith, P. *Polym. J.* **1985**, *17*, 117–132.
- (2) Tomalia, D. A. *New J. Chem.* **2012**, *36*, 264–281.
- (3) Tomalia, D. A. *Soft Matter* **2010**, *6*, 456–474.
- (4) Cheng, Y. Y.; Zhao, L. B.; Li, Y. W.; Xu, T. W. *Chem. Soc. Rev.* **2011**, *40*, 2673–2703.
- (5) Hu, J. J.; Xu, T. W.; Cheng, Y. Y. *Chem. Rev.* **2012**, *112*, 3856–3891.
- (6) Lee, C. C.; Mackay, J. A.; Frechet, J. M. J.; Szoka, F. C., Jr. *Nat. Biotechnol.* **2005**, *23*, 1517–1526.
- (7) Cohen, J. L.; Schubert, S.; Wich, P. R.; Cui, L.; Cohen, J. A.; Mynar, J. L.; Frechet, J. M. J. *Bioconjugate Chem.* **2011**, *22*, 1056–1065.
- (8) Ornelas-Megiatto, C.; Wich, P. R.; Frechet, J. M. J. *J. Am. Chem. Soc.* **2012**, *134*, 1902–1905.
- (9) Lee, Y.; Mo, H.; Koo, H.; Park, J. Y.; Cho, M. Y.; Jin, G. W.; Park, J. S. *Bioconjugate Chem.* **2007**, *18*, 13–18.
- (10) Tomalia, D. A. *Prog. Polym. Sci.* **2005**, *30*, 294–324.
- (11) Dufes, C.; Uchegbu, I. F.; Schatzlein, A. G. *Adv. Drug Delivery Rev.* **2005**, *57*, 2177–2202.
- (12) Tang, M. X.; Redemann, C. T.; Szoka, F. C., Jr. *Bioconjugate Chem.* **1996**, *7*, 703–714.
- (13) Nandy, B.; Maiti, P. K. *J. Phys. Chem. B* **2011**, *115*, 217–230.
- (14) Peng, S. F.; Su, C. J.; Wei, M. C.; Chen, C. Y.; Liao, Z. X.; Lee, P. W.; Chen, H. L.; Sung, H. W. *Biomaterials* **2010**, *31*, 5660–5670.
- (15) Xu, Q.; Wang, C. H.; Pack, D. W. *Curr. Pharm. Des.* **2010**, *16*, 2350–2368.
- (16) Ainalem, M. L.; Campbell, R. A.; Khalid, S.; Gillams, R. J.; Rennie, A. R.; Nylander, T. J. *J. Phys. Chem. B* **2010**, *114*, 7229–7244.
- (17) Svenson, S.; Tomalia, D. A. *Adv. Drug Delivery Rev.* **2005**, *57*, 2106–2129.
- (18) Liu, J.; Zhou, J.; Luo, Y. *Bioconjugate Chem.* **2012**, *23*, 174–183.

- (19) Kukowska-Latallo, J. F.; Bielinska, A. U.; Johnson, J.; Spindler, R.; Tomalia, D. A.; Baker, J. R., Jr. *Proc. Natl. Acad. Sci. U. S. A.* **1996**, *93*, 4897–4902.
- (20) Killops, K.; Campos, L. M.; Hawker, C. J. *J. Am. Chem. Soc.* **2008**, *130*, 5062–5064.
- (21) Santos, J. L.; Oliveira, H.; Pandita, D.; Rodrigues, J.; Pego, A. P.; Granja, P. L.; Tomas, H. *J. Controlled Release* **2010**, *144*, 55–64.
- (22) Luo, K.; Li, C.; Li, L.; She, W.; Wang, G.; Gu, Z. *Biomaterials* **2012**, *33*, 4917–4927.
- (23) Nam, H. Y.; Nam, K.; Hahn, H. J.; Kim, B. H.; Lim, H. J.; Kim, H. J.; Choi, J. S.; Park, J. S. *Biomaterials* **2009**, *30*, 665–673.
- (24) Kono, K.; Akiyama, H.; Takahashi, T.; Takagishi, T.; Harada, A. *Bioconjugate Chem.* **2005**, *16*, 208–214.
- (25) Sancliments, G.; Shen, H.; Giralto, E.; Albericio, F.; Saltzman, M. W.; Royo, M. *Biopolymers* **2005**, *80*, 800–814.
- (26) Kang, C.; Yuan, X.; Li, F.; Pu, P.; Yu, S.; Shen, C.; Zhang, Z.; Zhang, Y. *J. Biomed. Mater. Res., Part A* **2010**, *93*, 585–594.
- (27) Wada, K.; Arima, H.; Tsutsumi, T.; Chihara, Y.; Hattori, K.; Hirayama, F.; Uekama, K. *J. Controlled Release* **2005**, *104*, 397–413.
- (28) Arima, H.; Yamashita, S.; Mori, Y.; Hayashi, Y.; Motoyama, K.; Hattori, K.; Takeuchi, T.; Jono, H.; Ando, Y.; Hirayama, F.; Uekama, K. *J. Controlled Release* **2010**, *146*, 106–117.
- (29) Wada, K.; Arima, H.; Tsutsumi, T.; Hirayama, F.; Uekama, K. *Biol. Pharm. Bull.* **2005**, *28*, 500–505.
- (30) Zhang, Q.; Chen, S.; Zhuo, R. X.; Zhang, X. Z.; Cheng, S. X. *Bioconjugate Chem.* **2010**, *21*, 2086–2092.
- (31) Huang, R. Q.; Qu, Y. H.; Ke, W. L.; Zhu, J. H.; Pei, Y. Y.; Jiang, C. *FASEB J.* **2007**, *21*, 1117–1125.
- (32) Han, L.; Huang, R.; Li, J.; Liu, S.; Huang, S.; Jiang, C. *Biomaterials* **2011**, *32*, 1242–1252.
- (33) Cui, D.; Huang, P.; Zhang, C.; Ozkan, C. S.; Pan, B.; Xu, P. *J. Controlled Release* **2011**, *152* (Suppl1), e137–139.
- (34) Shan, Y.; Luo, T.; Peng, C.; Sheng, R.; Cao, A.; Cao, X.; Shen, M.; Guo, R.; Shi, X. Y. *Biomaterials* **2012**, *33*, 3025–3035.
- (35) Herrero, M. A.; Toma, F. M.; Al-Jamal, K. T.; Kostarelos, K.; Bianco, A.; Da, Ros, T.; Bano, F.; Casalis, L.; Scoles, G.; Prato, M. *J. Am. Chem. Soc.* **2009**, *131*, 9843–9848.
- (36) Breuing, M.; Lungwitz, U.; Liebl, R.; Goepferich, A. *Proc. Natl. Acad. Sci. U. S. A.* **2007**, *104*, 14454–14459.
- (37) Kihara, F.; Arima, H.; Tsutsumi, T.; Hirayama, F.; Uekama, K. *Bioconjugate Chem.* **2002**, *13*, 1211–1219.
- (38) Nam, H. Y.; Nam, K.; Lee, M.; Kim, S. W.; Bull, D. A. *J. Controlled Release* **2012**, *160*, 592–600.
- (39) Khan, M.; Ang, C. Y.; Wiradharma, N.; Yong, L. K.; Liu, S. Q.; Liu, L. H.; Gao, S. J.; Yang, Y. Y. *Biomaterials* **2012**, *33*, 4673–4680.
- (40) Hu, J. J.; Su, Y. Z.; Zhang, H. F.; Xu, T. W.; Cheng, Y. Y. *Biomaterials* **2011**, *32*, 9950–9959.